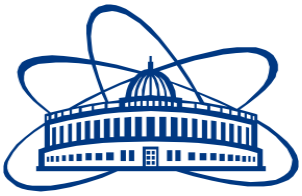

JOINT INSTITUTE FOR NUCLEAR RESEARCH
Flerov Laboratory of Nuclear Reactions

FINAL REPORT ON THE INTEREST PROGRAMME

Production and spectroscopic investigation of new neutron-rich isotopes near the neutron N=126 shell closure using the multinucleon transfer reactions

Supervisor
Mr. Viacheslav Vedeneev

Project By
Jaykumar Dipakbhai Patel
India, Gujarat University

Participation period
September 27 – November 5, Wave 5

Dubna, 2021

ABSTRACT

In the present article, data analysis of the Experimental data obtained from multinucleon transfer reaction $^{48}Ca+^{242}Pu$, $^{40}Ar+^{166}Er$, and $^{40}Ar+^{166}Er$ is performed. By doing so, spectroscopic investigation for different neutron rich isotopes around N =126 shell closure of Rn and Hg was made. Their production along with their daughter nuclides was speculated by studying their alpha decay spectrum obtained by plotting the experimental data. The data analysis included finding alpha decay peaks, finding out the isotope responsible for it, and mentioning different characteristics associated with that decay. For most of the peaks, a peak fitting analysis was performed to obtain precise Alpha decay energy, FWHM, and other peak parameters. With a direct connection of the research involved in the synthesis of Superheavy elements, the present work aims to bring out the spectroscopic evidence of the production of isotopes near the N= 126 region which is of great interest.

Contents

Chapter 1 - Introduction

1.1 Nuclies around N= 126 shell closure.

The Nuclear shell effects play a vital role in providing the stability to the nucleus giving rise to a higher lifetime or half-life of that nucleus against any decay. Similarly, for the super heavy nucleus to stay stable against its spontaneous decay or to have a larger lifetime it is assumed to be possible by the shell effects. Being said that, understanding this shell effect becomes a crucial prospect to know more about the stability provided to the Superheavy Elements. Thus, neutron rich isotopes around N= 126 shell closure are of great interest as they can provide a direct hint in the synthesis of superheavy elements. This could be in a way possible by understanding the decay of the nucleus around the shell closure produced via multinucleon transfer reactions[1]. In this project work, the experimental data from three full fusion multinucleon transfer reactions were therefore analyzed. The Nucleus in this region mainly decays by emitting alpha particles [1]and hence the discussion addressed in this work was completely based on studying the alpha spectrum obtained from the isotopes produced in the region N= 126 shell closure. The exact proportion of the nucleus decaying via any means of decay can be known from its 'Branching ratio'. Here in this work, for each nucleus, for both parent and daughter, its alpha branching ratio(here abbreviated as ABR) has been mentioned in its peak details. The number of alpha decays observed for a particular Isotope depicts its production in the particular reaction.

The MASHA(Mass Analyzer for superheavy atoms) setup having the resolution of 1700 mm using the ISOL(Isotope separation online)[2] method was employed in this type of reaction. In this method, the nuclear products produced in the fusion reaction with the target Nucleus in the hot catcher undergo ionization in the ECR source to Q = +1 state, after escaping from the graphite absorber[3]. After that, there is a silicon detector installed in the focal plane of the mass spectrometer to detect the decay of the nuclear products[3]. The frontal part of the detector consists of 192 strips along with other strips at different parts of the detector. Each strip can give a one-dimensional energy spectrum. Also, a Two-dimensional spectrum of the energy dependence on the strip number can be obtained in the form of a 2D -matrix[3]. In this project, both the alpha spectrum and the two-dimensional energy-position graph are discussed. Since the separation time of this method is 1.8±0.3 s [3], only those isotopes produced in the reaction having a larger life than the given separation time can be detected to undergo the alpha decay in the strip detector. The nuclear products of the fusion reaction have to undergo various processes before reaching the detector mentioned in[3]. which thereby hinders the possibility of detecting the short-lived isotopes produced in the fusion reaction. In this project, an effort is made to point out all the alpha decay in the alpha spectrum plotted. [4][5] was used to know more about the production of superheavy elements and their chemistry.

1.2 Project goals and scope of the work

The goal of the project is to perform the data analysis of the experimental data obtained from full fusion multinucleon transfer reactions and bring out the alpha decay peaks observed in the spectrum plot. The task considered is to find out the responsible isotope for that particular alpha decay energy with other properties of decay using the chart of Nuclides and decay chains. The scope of the work was restricted to be considering and investigating only the alpha decay chain of the nucleus. Moreover, peak analysis was not performed for all the peaks in the spectrum. The two-dimensional Energy-position graph was also obtained by plotting the matrix data as heatmap and performing detector calibration for all the three multi nucleon transfer reactions.

Chapter 2 - Data Analysis of the Experimental data

2.1 Spectroscopic evidence from MNTR - ^{48}Ca +^{242}Pu using alpha decay chains of the decaying Isotopes

The peaks in the alpha spectrum for different Isotopes were searched based on the Energy of their alpha decay observed in their decay chains. The presence of a particular type of alpha decay energy peak in the spectrum speculates the production of the particular Isotopes which has that alpha decay energy in its decay chain. Here below the production of the Rn Isotopes is discussed and Peak analysis of the prominent peak is also performed.

2.1.1 - Production of ^{212}Rn

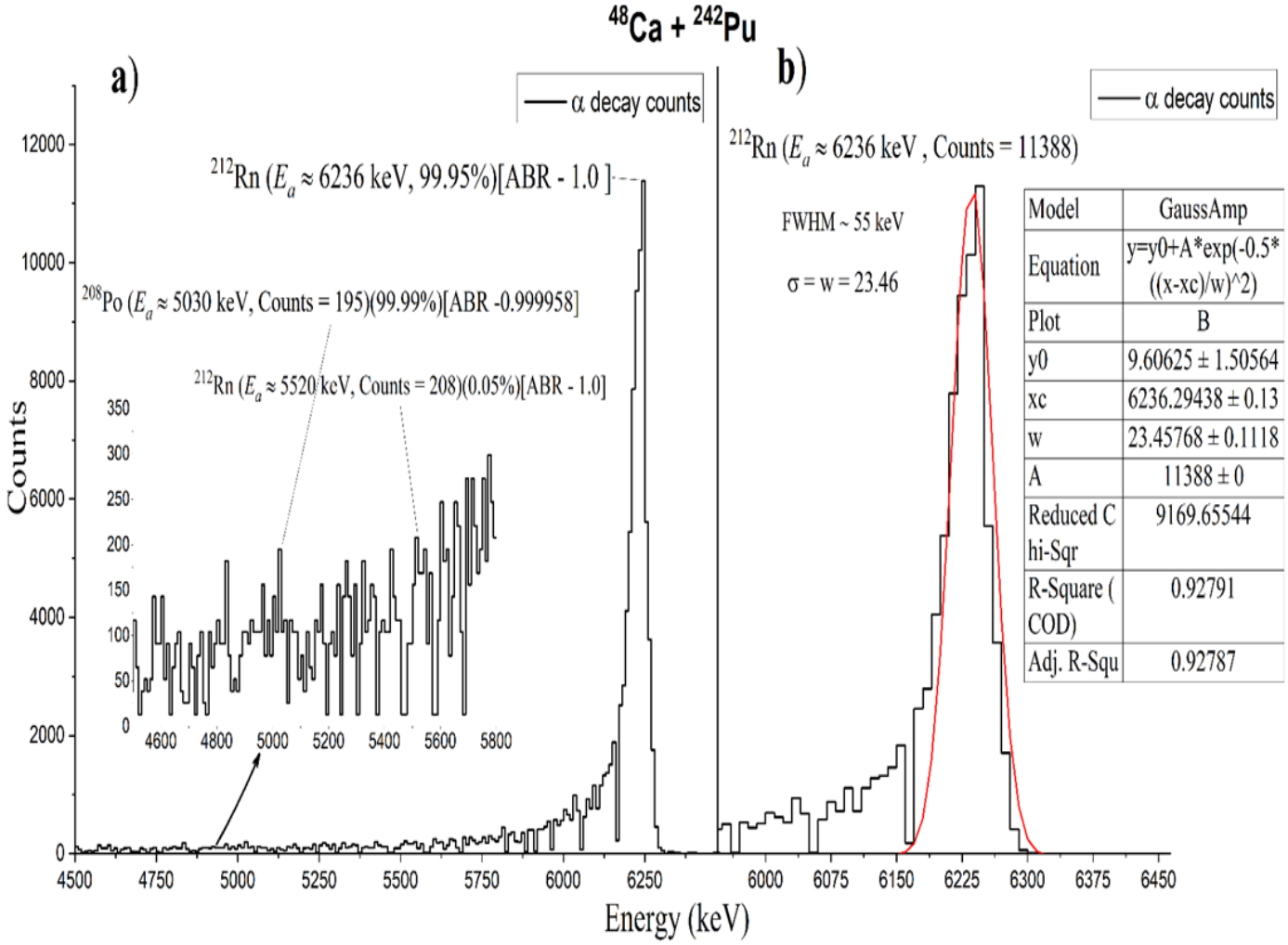

Figure 2-1: a) the alpha decay peaks observed in the spectrum of ^{212}Rn parent Isotopes and its daughter isotopes are highlighted along with their energies and other parameters of that decay. b) Peak analysis of the Prominent peak in the alpha energy spectrum is performed.

The peaks are shown in the above figure2-1 for example " ^{212}Rn ($E_a \approx 6236$ keV, 99.95%)[ABR - 1.0]" could be explained as follows:

- Here, 'Ea ≈ 6236 keV' shows the alpha decay energy of the alpha particle emitted from the Isotope ^{212}Rn.
- As there are different alpha decay energy possible for the Isotope to undergo alpha decay, the value here, '99.95%' shows the percentage of probability that the alpha particle decay from the Isotope would have that particular energy of decay. i.e., here it is 6236 keV.
- Here 'ABR' means Alpha Branching Ratio for that exact Nucleus (here – ^{212}Rn). This fraction indicates the probability of that Isotope undergoing a particular type of decay. As here 'ABR – 1.0' tells that the Nucleus ^{212}Rn will undergo decay 100 percent via emitting the alpha particle or will have only alpha decay and not any other type of mode of decay.
- On the plot where peak fitting is shown, the peak with its energy and total counts is also mentioned along with the peak parameters. The above-mentioned points are followed for all the alpha spectrum analysis done in this project.

Discussing the ^{212}Rn alpha spectrum the most prominent alpha decay observed was of energy equal to 6264 keV as given in the standard Chart of Nuclides, however, the peak observed corresponds to that at 6236 keV as seen in above figure 2-1. The decay energy of the alpha particle is not always fixed as some nucleons may carry different alpha energy. This type of small energy fluctuations in the alpha decay energy is noticed in most of the decays going to be discussed ahead. The peak parameters are given in figure 2-1 b) are given with their respective standard errors. The fitting function used was GaussAmp to get the best fit of the peak. The alpha decay from ^{208}Po at energy 5114.9 keV is observed at around 5030 keV and another decay of ^{212}Rn which is very less probable is observed at 5520 keV. The lifetime of ^{212}Rn is 23.9 minutes and 2.89 years for ^{208}Po Isotope. This is high enough than the separation time by the ISOL method which is about 1.8±0.3 s [3].

2.1.2 Production of ^{218}Rn

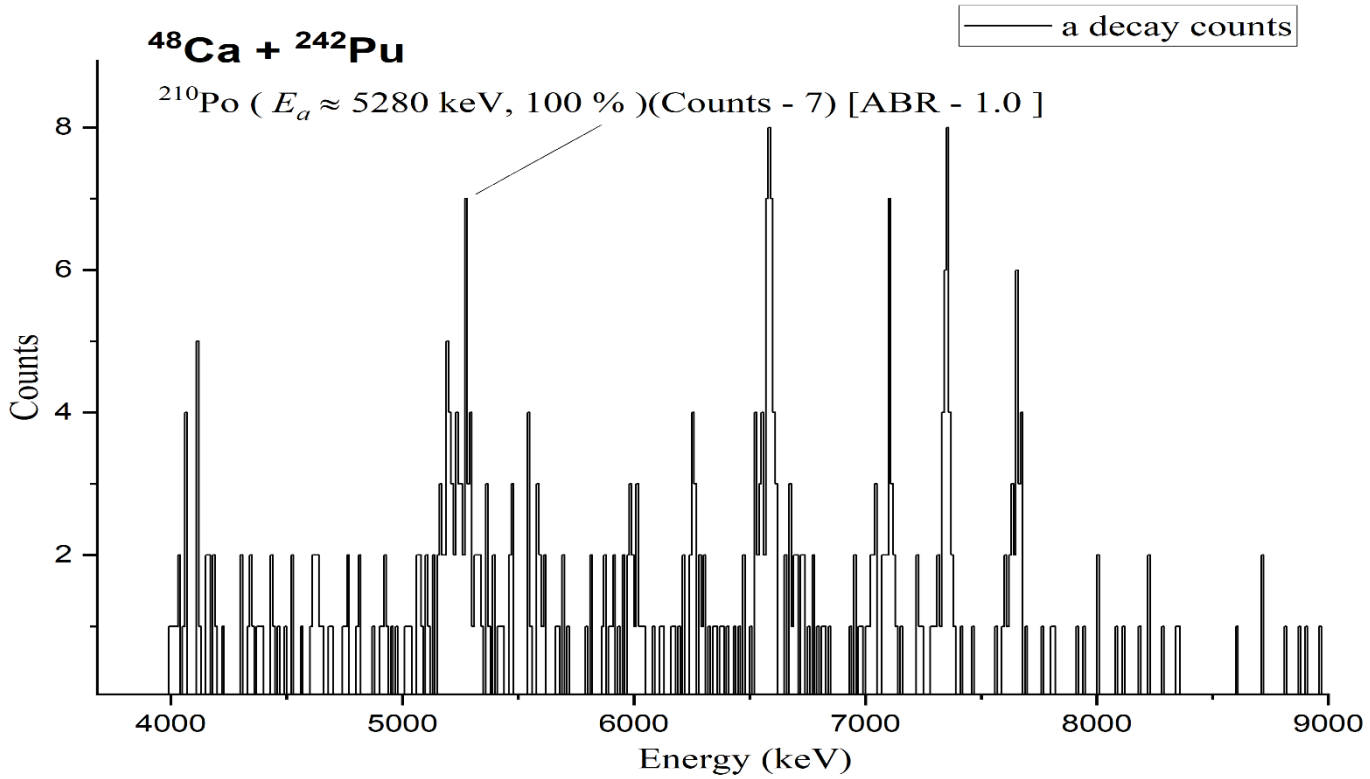

Figure 2-2 : Alpha spectrum for ^{218}Rn Isotope and its decay products.

Here above in Figure 2-2, the alpha decay of ^{218}Rn and ^{214}Po isotopes could not be seen. Instead, the alpha decay of its daughter nucleus can be seen. This is because of the very less lifetime of the ^{218}Rn and ^{214}Po nucleus which is 35 ms and 164.3 us respectively as given in the Chart of Nuclide. This is very less than the time of separation taken by the ISOL method and hence the peaks of those are not observed. Moreover, the data here is from the single strip of the detector located in the area of 218 mass separation region and hence the counts detected and peaked are very less and are close to the background. However, because of the large lifetime of the daughter nucleus ^{210}Po which is 138.376 days, its alpha decay energy ^{210}Po(E_a =5304.33 keV)is observed at 5280 keV approximately.

2.1.3 Production of ^{219}Rn

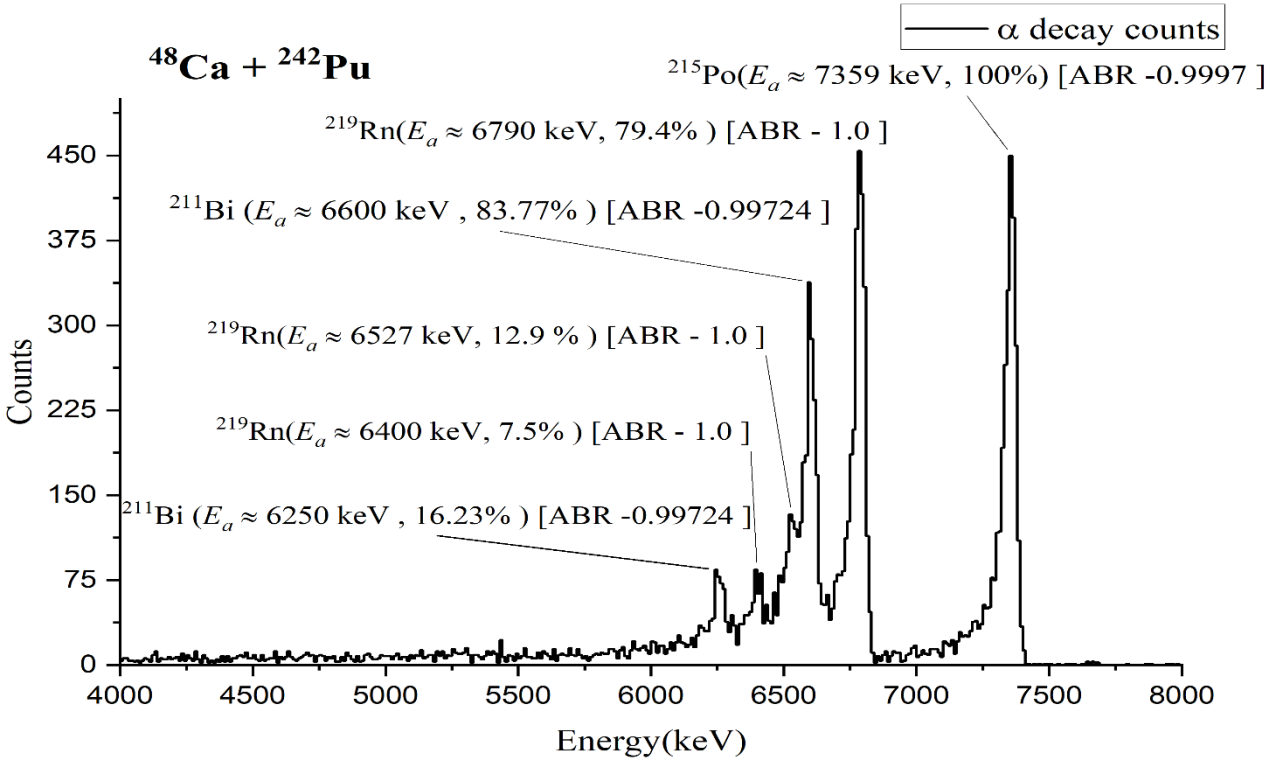

Figure 2-3 : Alpha spectrum for ^{219}Rn Isotope and its decay products.

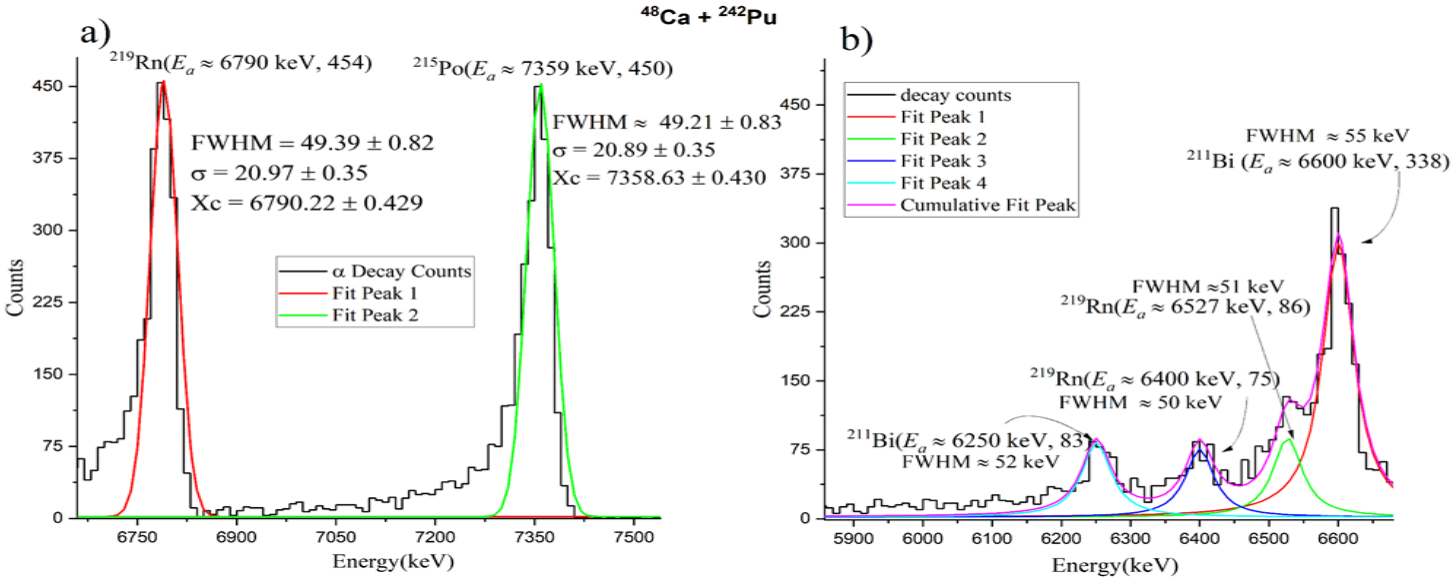

Figure 2-4: a) shows the peak analysis performed for the most prominent peaks of the ^{219}Rn alpha spectrum. b) shows the peak analysis for the other irregular peaks of the spectrum

In the above figure, 2-3 and 2-4 alpha spectrum giving evidence of the production of ^{219}Rn(3.96 s) and daughter nucleus ^{215}Po(1.78ms) and ^{211}Bi(2.14 min) can be seen. The most prominent alpha decay observed was of ^{219}Rn($E_a \approx 6819$ keV) which in the present spectrum peaked at 6790 keV. The other two alpha decay of ^{219}Rn(Ea ≈ 6552.6 keV) and ^{219}Rn(Ea ≈ 6425.0 keV) were peaked at approximately 6527 keV and 6400 keV respectively. However, these peaks were not observed to be separated well from the background or other peaks, and hence good fit of those peaks was not obtained(Adj. R^2 = 0.235)(peak type -Lorentz). The prominent peaks had a quite good fitting possible(Adj. R^2 = 0.679)(peak type – GaussAmp) as seen in Figure 2-4 a). The daughter peaks included of ^{215}Po(Ea ≈ 7386.1 keV), ^{211}Bi((Ea ≈ 6622.9 keV), and ^{211}Bi((Ea ≈ 6278.2 keV) were peaked at 7358 keV, 6600 keV, and 6250 keV respectively as seen in figure 2-3. Alpha decay from ^{211}Po(0.5 s) being a part of the decay chain of ^{219}Rn was not observed in the given alpha spectrum.

2.1.4 Heatmap for Rn Isotopes.

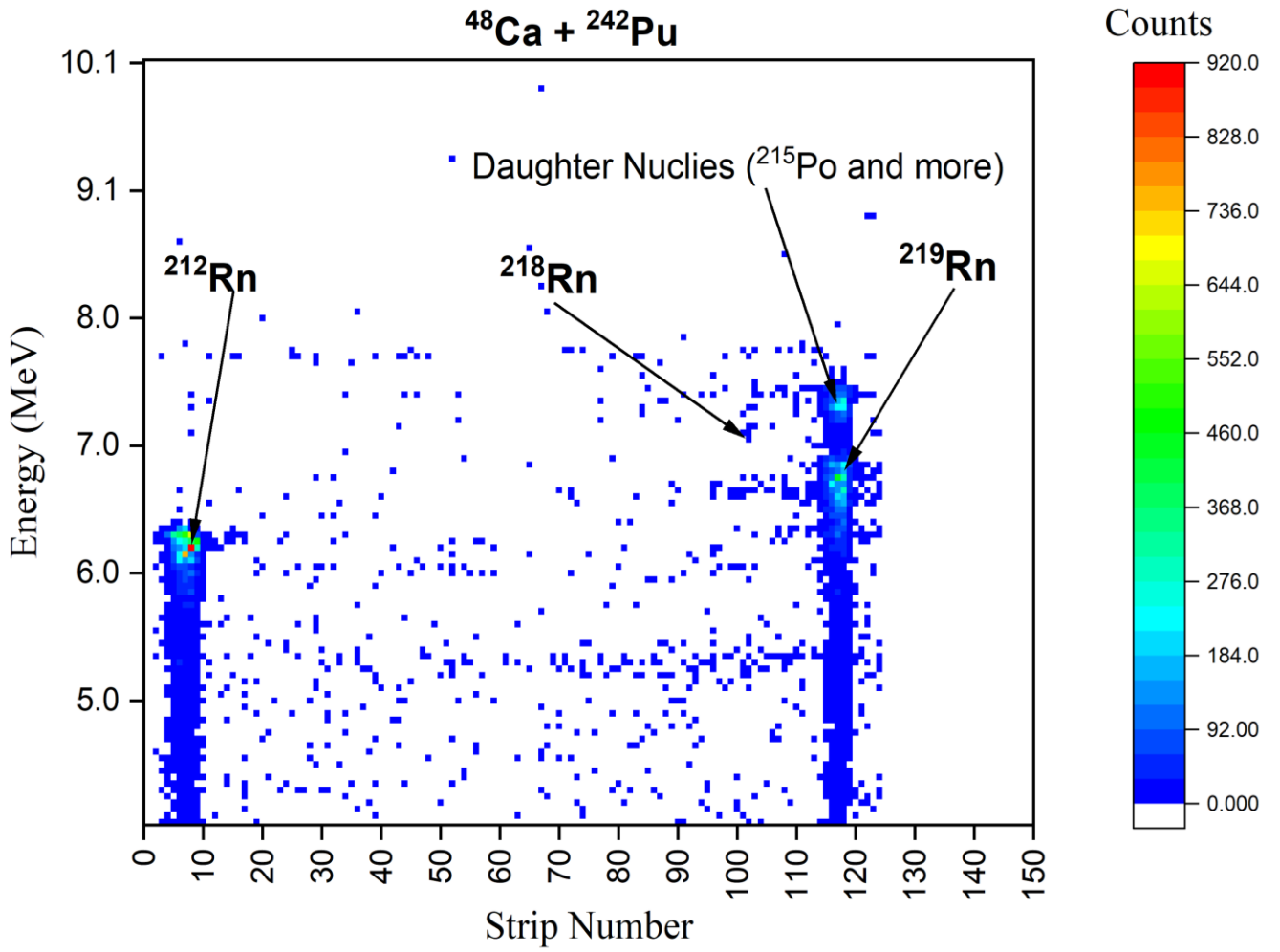

Figure 2-5: Two-dimensional energy-position graph for Rn isotopes with mass numbers from 212 to 219.

Production of Rn isotopes in the multinucleon transfer reaction ^{48}Ca +^{242}Pu positioned with at respective Detector strip number can be seen in the above figure2-5. The huge gap between ^{212}Rn and ^{219}Rn Isotope visible products obtained from the fusion reaction can be explained. From 213 to 217 mass number of Rn isotopes, the lifetime is very less than the separation time which is 1.8±0.3 s [3]. Thus, the Isotopes in between are not visible as they do not live long to reach the ECR ion source itself. Even the ^{218}Rn is barely visible with a lifetime of 35 ms The above Heatmap was obtained by performing detector calibration.

2.2 Spectroscopic evidence from MNTR – ^{40}Ar +^{166}Er using alpha decay chains of the decaying Isotopes.

The spectroscopic evidence of the production of ^{201}Rn to ^{205}Rn shall be discussed in this section. Further, the two-dimensional energy-position graph for this range of isotopes produced in this multinucleon transfer reaction ^{40}Ar +^{166}Er will be too discussed. It was evident that some of the data contained the negative counts, thereby here they were treated as the background noise and hence are not included in the alpha spectrum plotted.

2.2.1 Production of ^{201}Rn

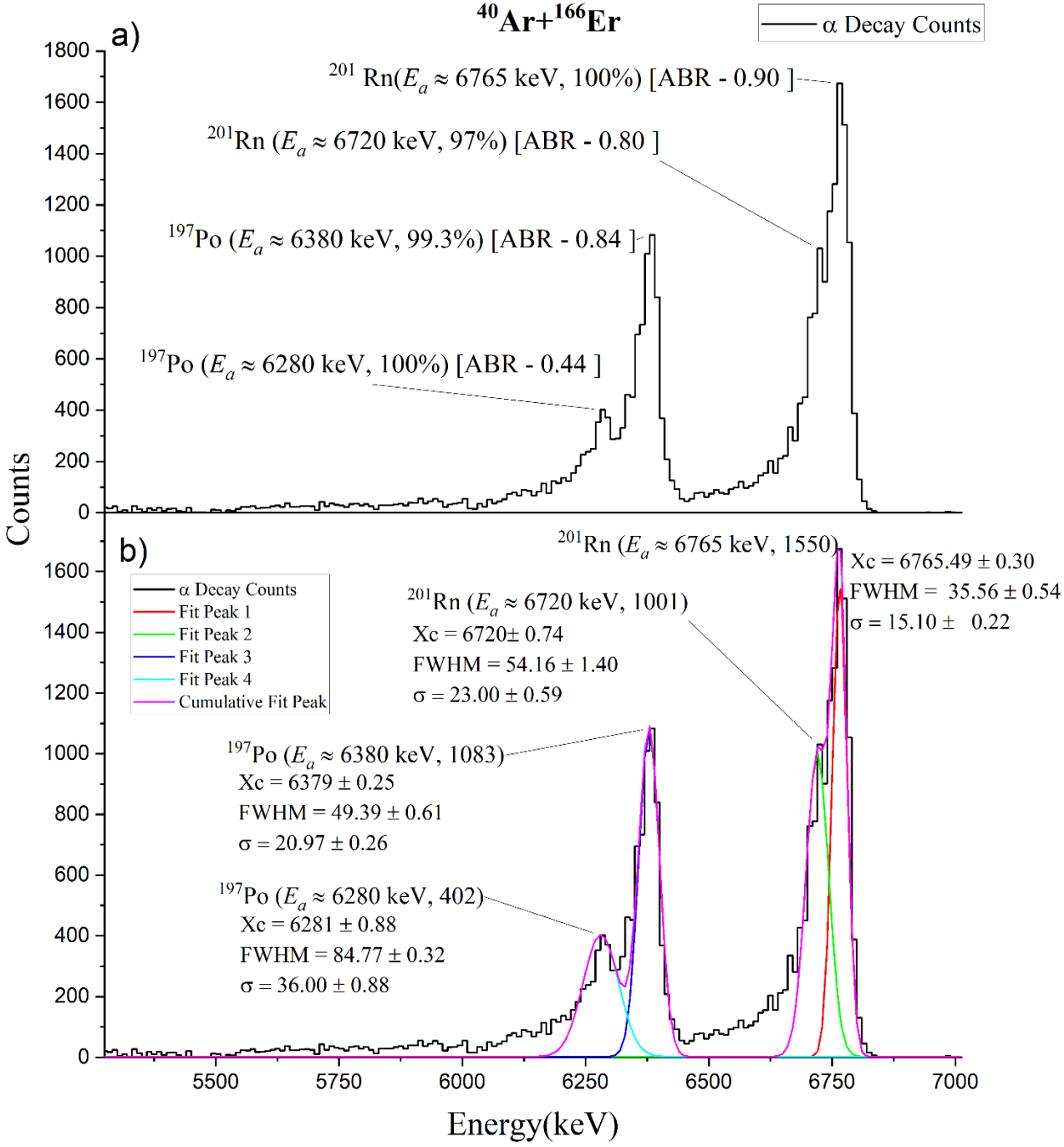

Figure 2-6: Alpha spectrum of ^{201}Rn. a) shows the peaks identified in the spectrum and its different specifications. b) shows the peak analysis performed for the given spectrum and its properties

In the above alpha spectrum of ^{201}Rn, the alpha decay from isotope ^{201}Rn(7.1 s) and ^{201}Rn(3.8 s) having two different lifetimes were observed. Alpha decay from the former with a larger lifetime ^{201}Rn(Ea ≈ 6725 keV) was peaked at 6720 keV and for later cases with a lower lifetime ^{201}Rn(Ea ≈ 6773 keV) was peaked at 6765 keV. The alpha decay from the only possible daughter of ^{201}Rn which is ^{197}Po(53.6 s) and ^{197}Po(25.8 s) was also observed. That is decay from ^{197}Po(Ea ≈ 6281 keV)(53.6 s) was observed at 6280 keV and the alpha decay ^{197}Po(Ea ≈ 6383 keV)(25.8 s) was peaked at 6380 keV approximately. The fitting performed here was with the GaussAmp peak fit and the Adj. R^2 value obtained was 0.94672. Since the energies of the two ^{201}Rn decays are very near two each other, the peaks of those as seen in Figure 2-6 a) are not well separated.

2.2.2 Production of ^{202}Rn

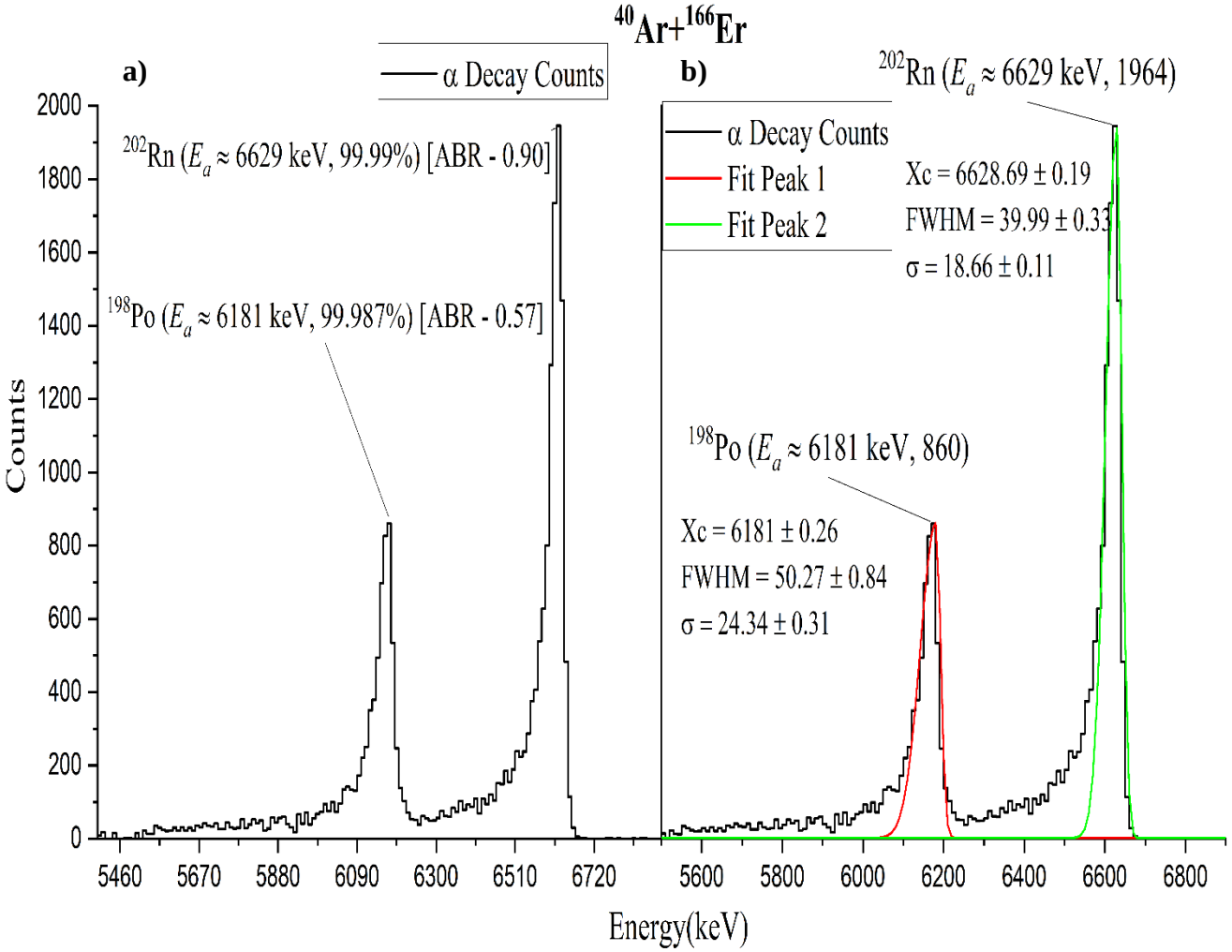

Figure 2-7 : Alpha spectrum of ^{202}Rn. a) shows the peaks identified in the spectrum and its different properties . b) shows the peak analysis performed for the given spectrum of ^{202}Rn

In the alpha spectrum of ^{202}Rn(10.0 s), only two prominent decays could be seen. ^{202}Rn decays to two possible daughters, one is ^{202}At(184 s) and ^{198}Po(1.77 min). However, the alpha decay from ^{202}At was not observed or could be barely seen in this above alpha spectrum. The alpha decay of ^{202}Rn(Ea ≈ 6639.5 keV) is peaked at 6629 keV and the alpha decay of ^{198}Po(Ea ≈ 6182.0 keV) is peaked at 6181 keV as seen in the above figure 2-7 a). The peak fitting function here used was again GaussAmp and the Adj. R^2 obtained was 0.93008 which is a quite good fit obtained.

2.2.3 Production of ^{203}Rn

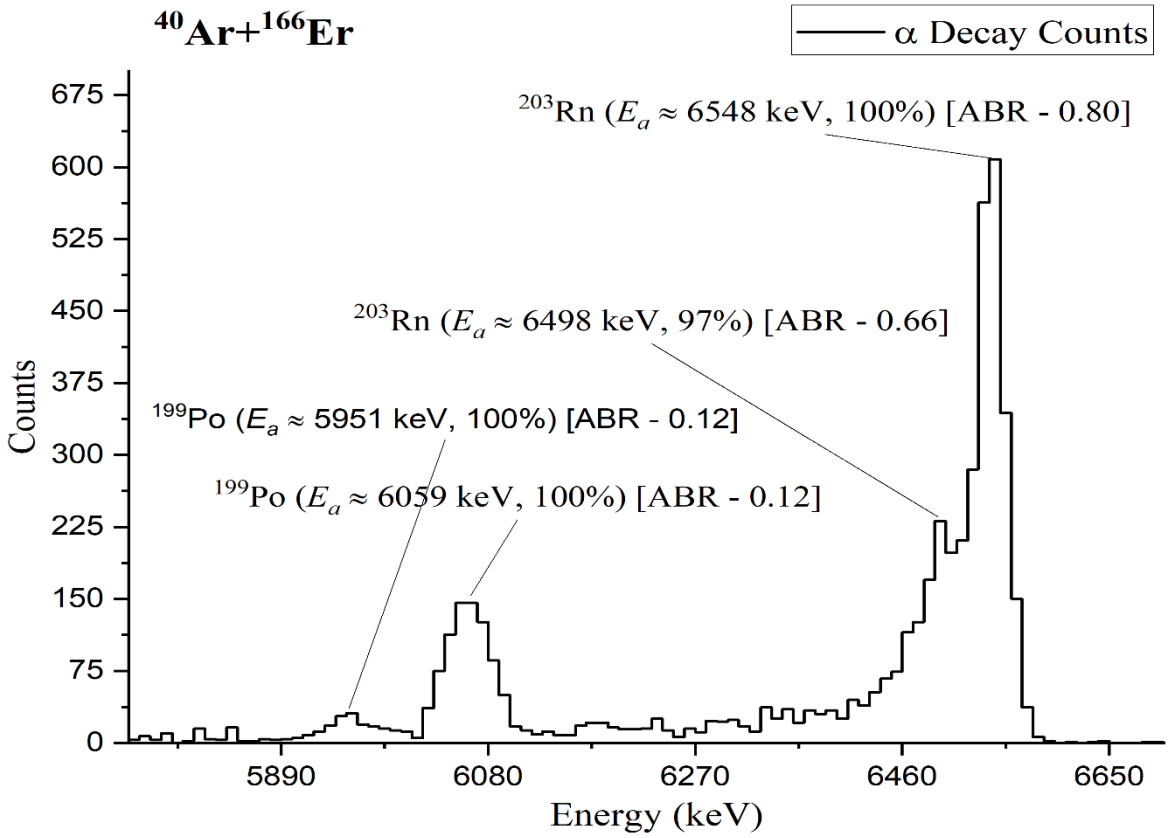

Figure 2-8 : Alpha spectrum of ^{203}Rn

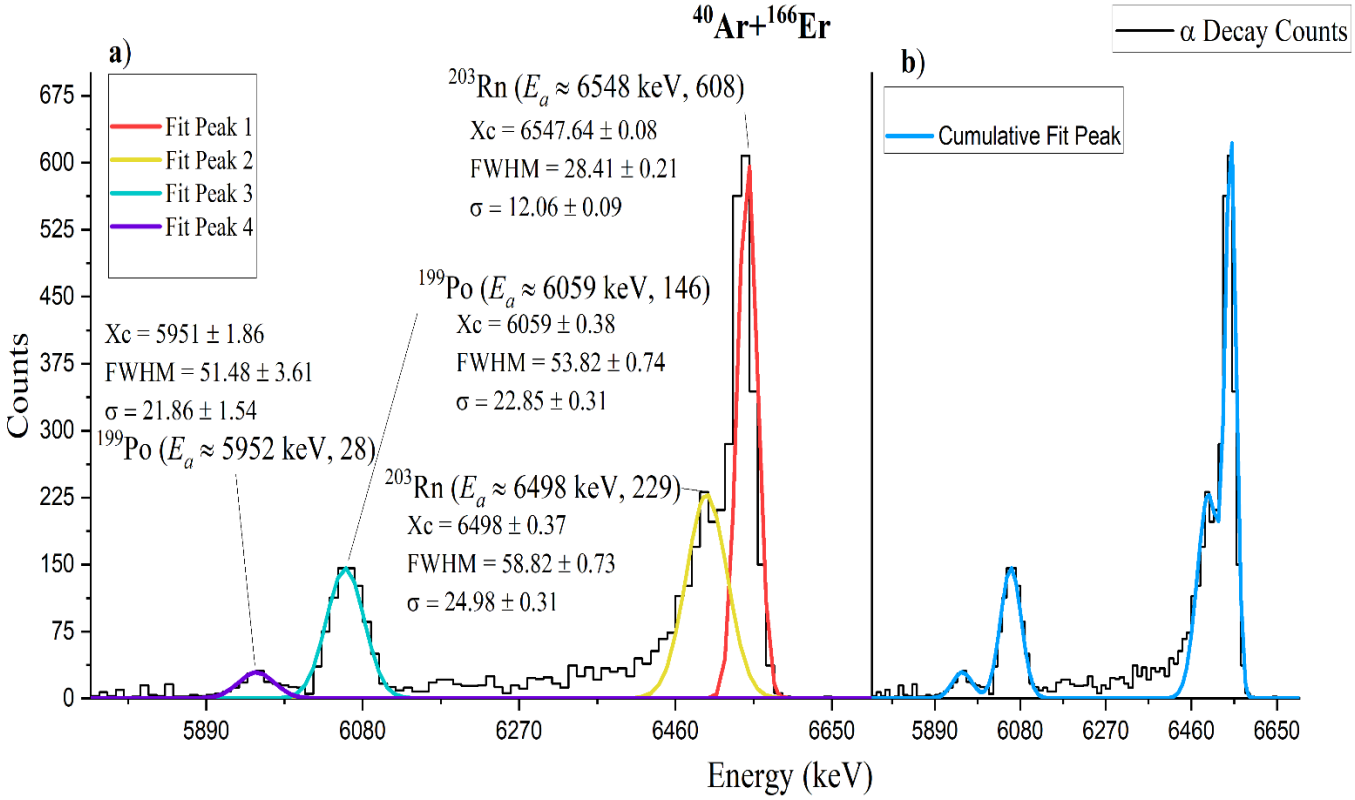

Figure 2-9: Peak Analysis of ^{203}Rn spectrum. a) Individual peak fit and its parameters can be seen. b) Cumulative fit is shown.

Here again, the alpha decay from the ^{203}Rn isotope having different lifetimes ^{203}Rn(28 s) and ^{203}Rn(45 s) can be seen in the above Figure 2-9 a). The alpha decay from ^{203}Rn($E_a \approx 6549.0$ keV) (28 s) was observed at energy approximately equal to 6548 keV. And from ^{203}Rn($E_a \approx 6499.3.0$ keV)(45 s) was observed at 6498 keV approximately. Since the two alpha decay energy is too close, the two distinguished peaks of those could not be seen. The two other alpha decay peaks of the daughter nucleus ^{199}Po ($E_a \approx 5952$ keV) (5.48 min) and ^{199}Po($E_a \approx 6059$ keV) (4.17 min) was observed at 5951 keV and 6059 keV respectively. The fitting function used here was the GaussAmp and the Adj.R^2 was obtained s 0.9606 which is a very good fit.

2.2.4 Production of ^{204}Rn

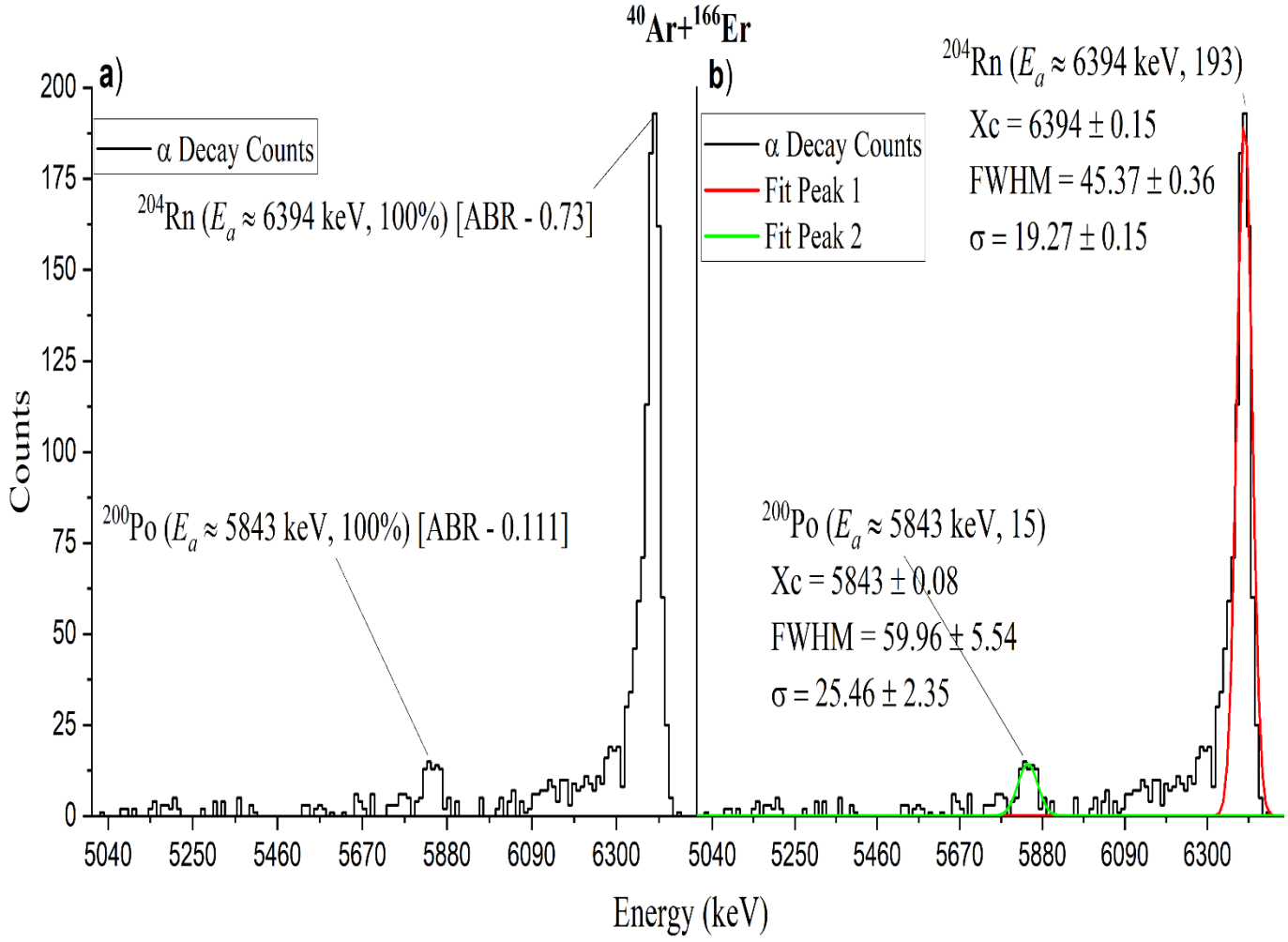

Figure 2-10: Alpha spectrum of ^{204}Rn. a) shows the peaks identified in the spectrum and their different properties. b) shows the peak analysis performed for the given spectrum of ^{204}Rn

Here, only two alpha decay prominent enough to be called peaks are observed in the alpha spectrum of ^{204}Rn isotope. The alpha decay from ^{204}Rn(Ea ≈ 6418.9 keV) is peaked at 6394 keV and the alpha decay of ^{198}Po(Ea ≈ 5861.9 keV)(11.5 min) is peaked at 5843 keV approximately as seen in the above figure 2-7 a).
The percentage probability for the alpha decay shown in the above spectrum was not mentioned in the chart of nuclides. however, as there was no other alpha decay energy for the ^{204}Rn to decay, it was here taken as 100 percent. The fitting function used as GaussAmp and the Adj.R^2 obtained was 0.8813. Since the ABR of ^{200}Po for alpha decay is very low compared to that of its parent nucleus, a significant difference in the counts of the alpha peaks can be seen in Figure 2-10 b).

2.2.5 Production of ^{205}Rn

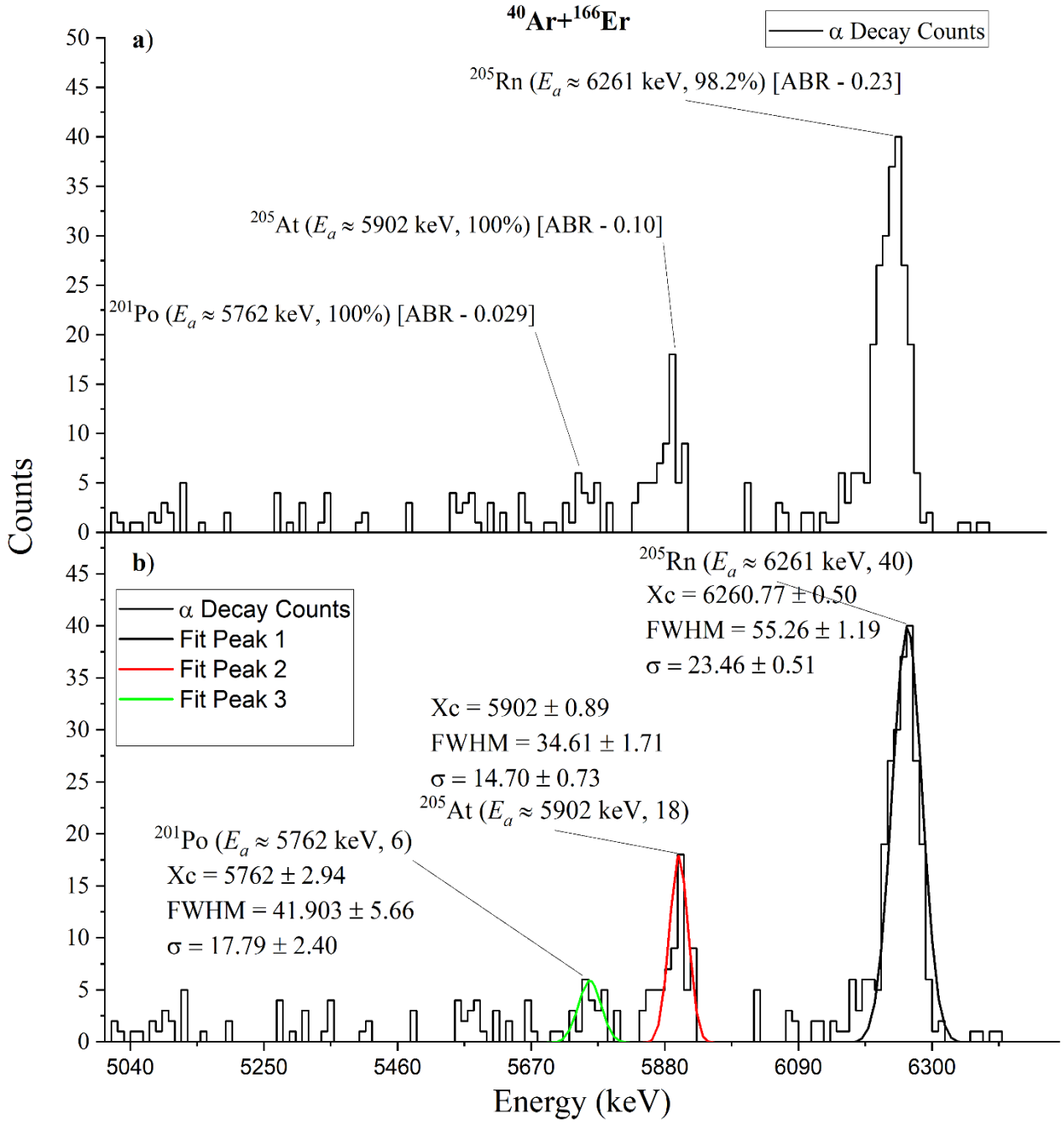

Figure 2-11: Alpha spectrum of ^{205}Rn. a) shows the peaks identified in the spectrum and their different properties. b) shows the peak analysis performed for the given spectrum of ^{205}Rn

From above Figure 2-11 a), it is evident that the alpha decay of the daughter nucleus of ^{205}Rn was not observed well, i.e., the peaks were not peaked properly and hence larger standard error could be seen in the smaller and irregular peaks. Also, the overall counts of the spectrum were low- speculating the lesser cross-section of ^{205}Rn production in the ^{40}Ar+^{166}Er MNTR. The most prominent peak of ^{205}Rn($E_a \approx 6262.0$ keV) is observed to be peaked at approximately 6261 keV. The peaks for the daughter Nucleus ^{205}At($E_a \approx 5902$ keV) is peaked at approximately 5902 keV which is quite very accurate as compared to previous cases. And for ^{201}Po($E_a \approx$ 5786 keV) was peaked at approximately 5762 keV. The fit performed here is again a GaussAmp peak fit and the value of the Adj. R^2 is 0.509. This degraded goodness of fit could be explained by the irregular peaks present in the alpha spectrum.

2.2.6 Heatmap for Rn Isotopes (A = 100 to A =106)

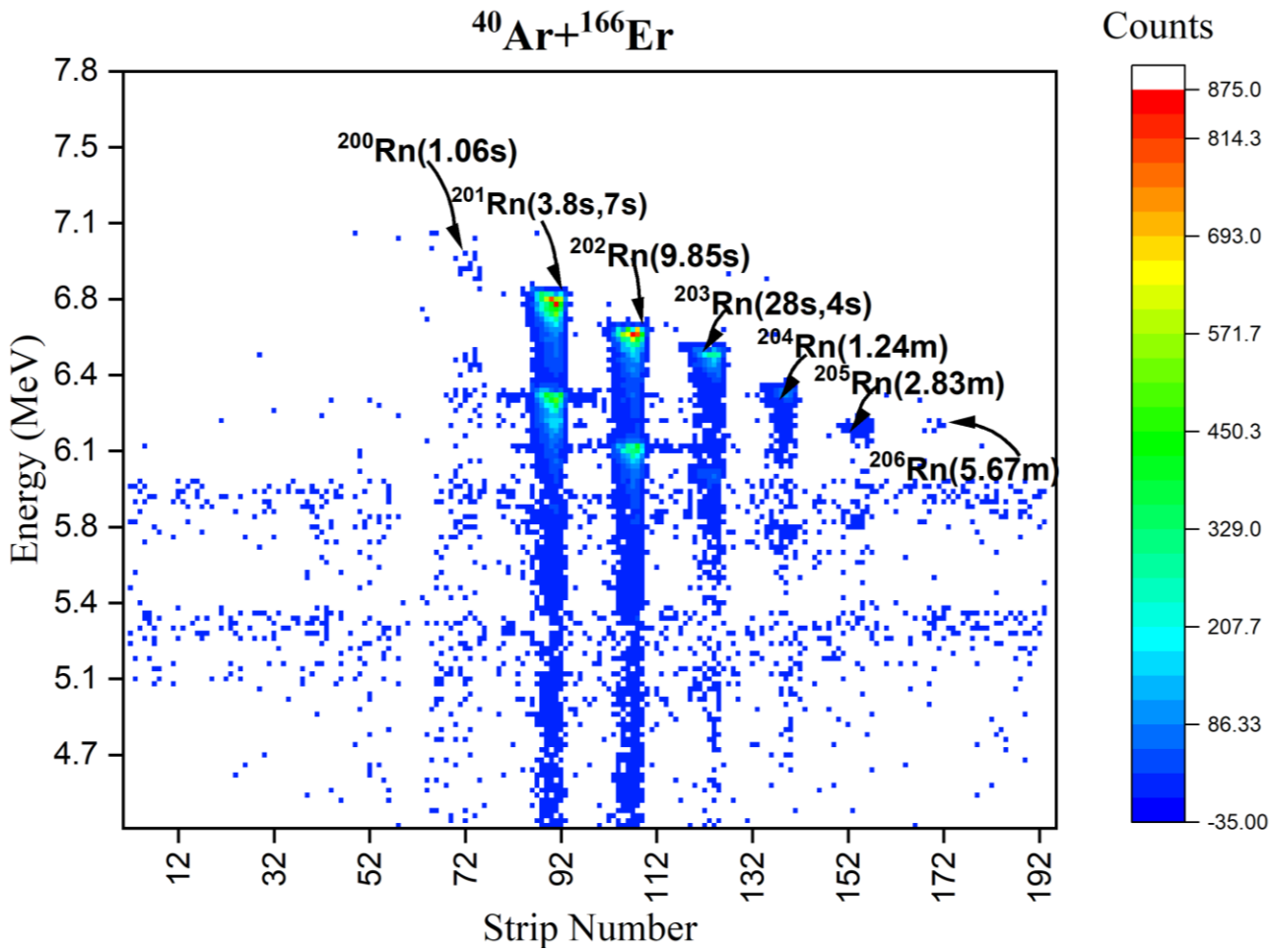

Figure 2-12: Two-dimensional energy-position graph for Rn isotopes with mass numbers from 200 to 206.

In the above Figure 2-12, the production of various Rn Isotopes along the detector strip number can be seen. The Y-axis shows the energy corresponding to the alpha decays of the respective isotopes. As seen, the ^{201}Rn and ^{202}Rn isotopes are largely produced in the multinucleon transfer reaction ^{40}Ar+^{166}Er. The above plot was obtained using the Rn -matrix provided in the experimental data. The counts less than 1 were neglected in creating the above heatmap for better viewing of the results.

2.3 Spectroscopic evidence from MNTR – ^{40}Ar +^{148}Sm using alpha decay chains of the decaying Isotopes.

Here, in this section production of Mercury(Hg) isotopes from mass number A = 180 to 185 would be discussed. Meanwhile, the negative counts present in the spectral data were neglected as considered as a background. The negative counts occurring at certain energies were also checked if they resemble some alpha decay energy of the decaying isotope in the alpha decay chain of the parent isotope.

2.3.1 Production of ^{180}Hg

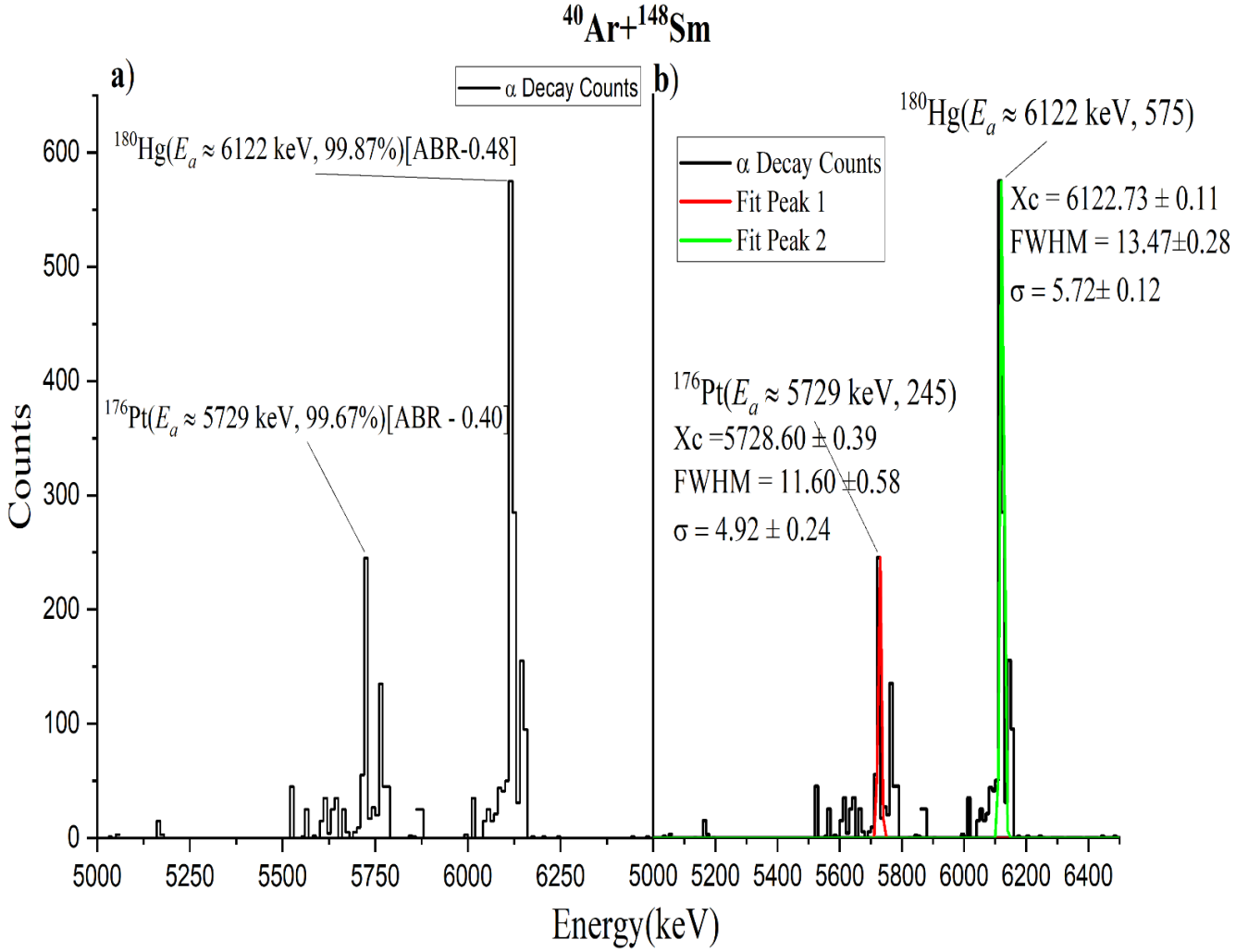

Figure 2-11: Alpha spectrum of ^{180}Hg. a) shows the peaks identified in the spectrum and their different properties. b) shows the peak analysis performed for the given spectrum of ^{180}Hg

The alpha decay peaks in the spectrum of ^{180}Hg can be seen in the above figure 2-11 a). Here, only two prominent peaks were identified as the alpha decay peaks. That is, one from ^{180}Hg($E_a \approx 6119$ keV)(2.58 s) was peaked at approximately 6122 keV and from ^{176}Pt($E_a \approx 5730$ keV)(6.3 s) was peaked at 5729 keV approximately. Here the alpha decay peaks were not properly shaped and hence the good fit was not obtained resulting in Adj. $R^2 = 0.7118$ with GaussAmp fit. Some other peak-like structures could also be seen around 5750 keV and in some other regions. But there was no kind of alpha decay energy resembling that in the decay chain of the Parent as well as Daughter Nucleus. Peak parameters can be seen in Figure 2-11 b) along with their respective standard errors.

2.3.2 Production of ^{181}Hg

The three primary daughters of ^{181}Hg(3.54 s) as seen in the decay chain of it are ^{181}Au(14.5 s), ^{180}Pt(56 s), and ^{177}Pt(11 s). However, as seen in the below Figure 2-12 no alpha decay from the ^{181}Au as well as ^{180}Pt could be seen due to very low ABR. Only from ^{177}Pt($E_a \approx 5517$ keV) alpha decay with very few counts was observed at 5510 keV. The rest two peaks were of ^{181}Hg($E_a \approx 6006$ keV) and ^{181}Hg($E_a \approx 5938$ keV) was obtained at 5990 keV and 5948 keV respectively. The rest of the peak analysis for the major peaks can be seen in the below figure 2-12 b). The peaks are not properly shaped and hence are irregular. Therefore, the goodness of fit obtained with the GaussAmp peak fit function was 0.639 only. There was no alpha decay energy found corresponding to counts seen at around 5600 keV and 5700 keV.

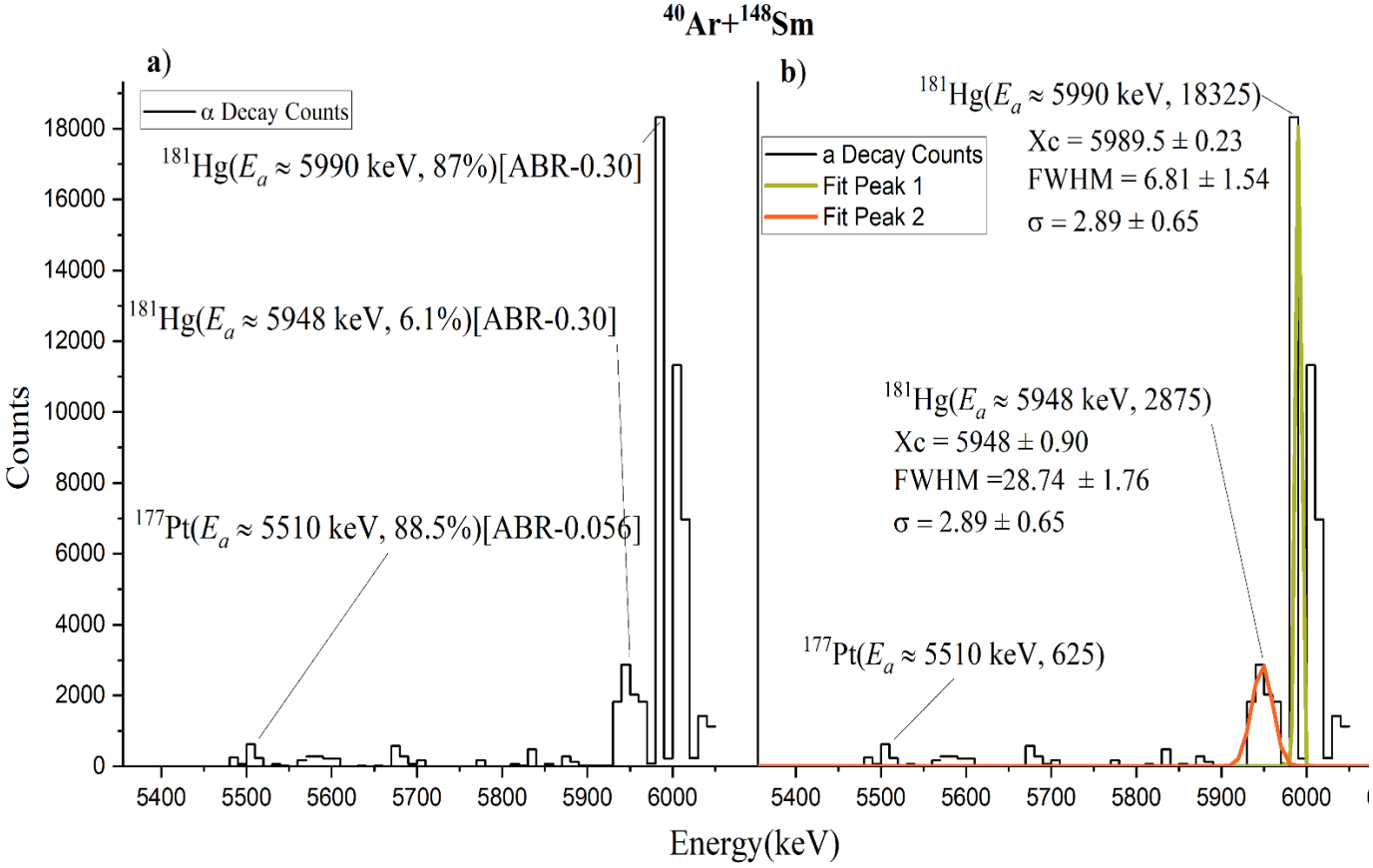

Figure 2-12 : Alpha spectrum of ^{181}Hg. a) shows the peaks identified in the spectrum and its different properties . b) shows the peak analysis performed for the given spectrum of ^{181}Hg

2.3.3 Production of ^{182}Hg

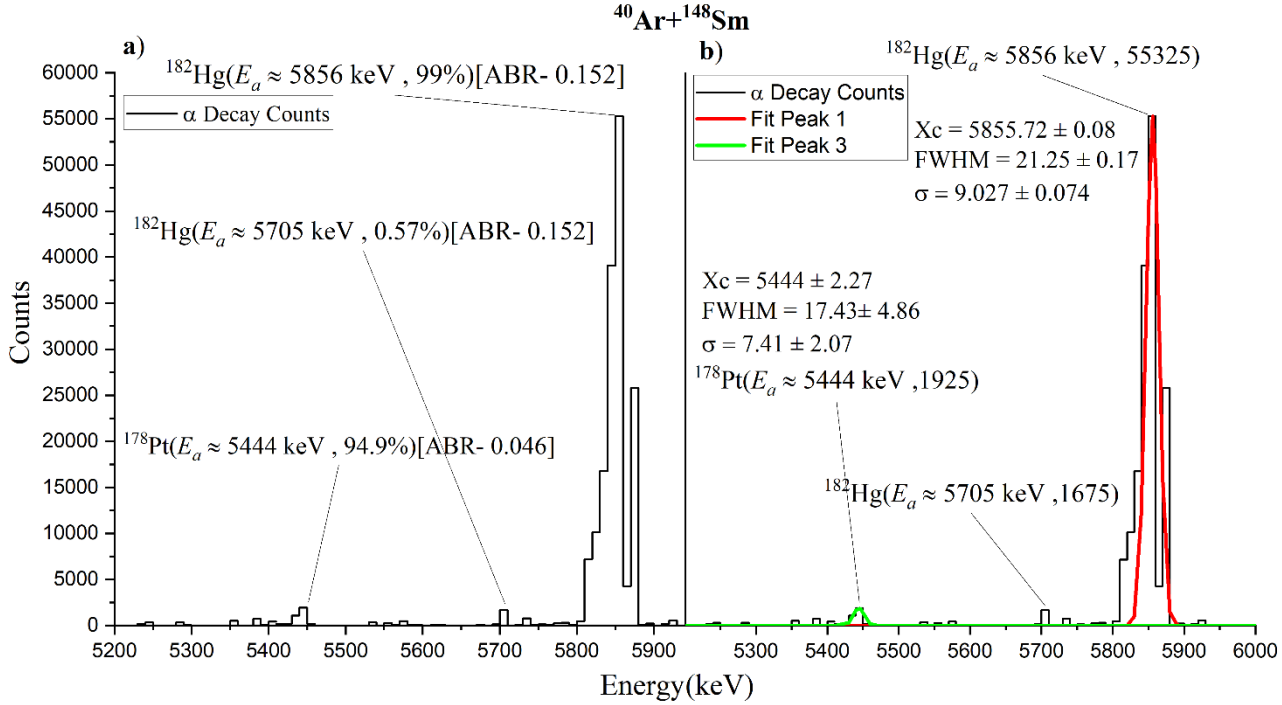

Figure 2-13: a) Shows the alpha spectrum of ^{182}Hg and its identified peaks of the spectrum along with its properties of decay. b) Peak analysis for the ^{182}Hg alpha spectrum and its peak parameters.

The major alpha decay observed from the ^{182}Hg((E_a ≈ 5867 keV) observed at 5856 keV approximately.

The other two decays observed were very low as compared to the prominent peak of the spectrum, however, if seen 'counts', they were not less as seen in previous cases. Hence alpha decay of ^{182}Hg(($E_a \approx 5700$ keV) and from ^{178}Pt($E_a \approx 5446$ keV) (21.1 s) were marked at 5705 keV and 5444 keV respectively. The peak fitting was performed for only quiet well-shaped peaks and hence with GaussAmp fit, the Adj.R^2 obtained was 0.8275.

2.3.4 Production of ^{183}Hg

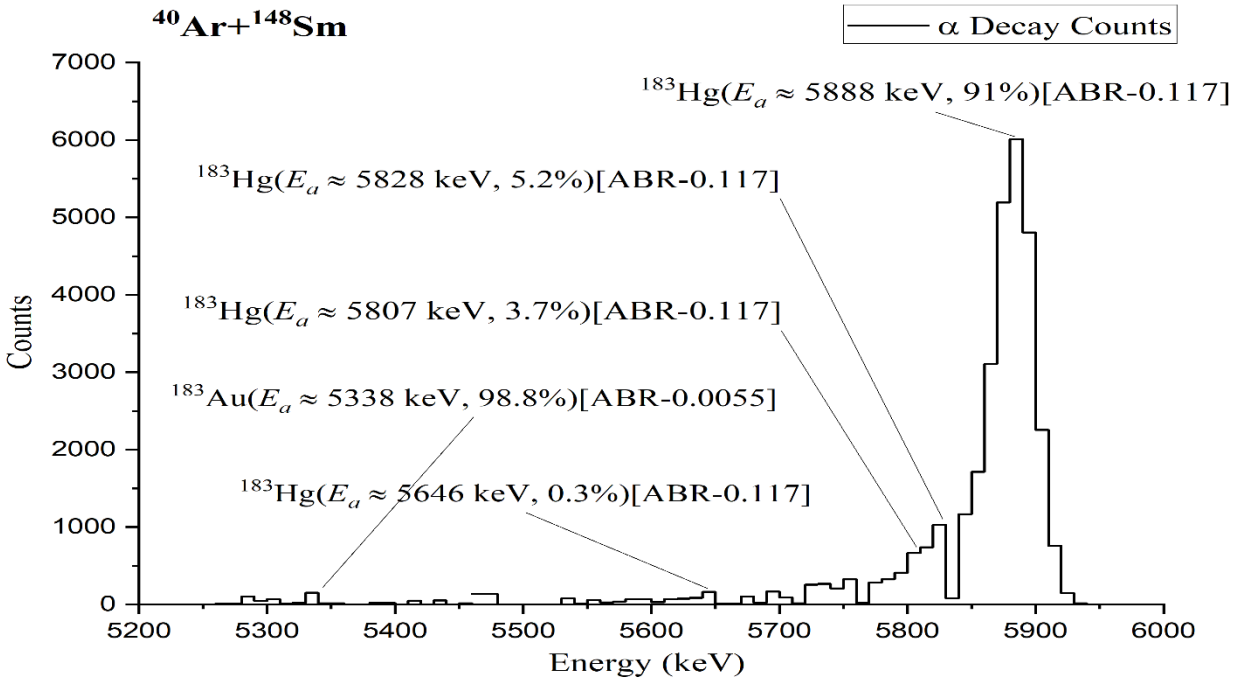

Figure 2-14: Alpha spectrum of ^{183}Hg and its identified alpha decay.

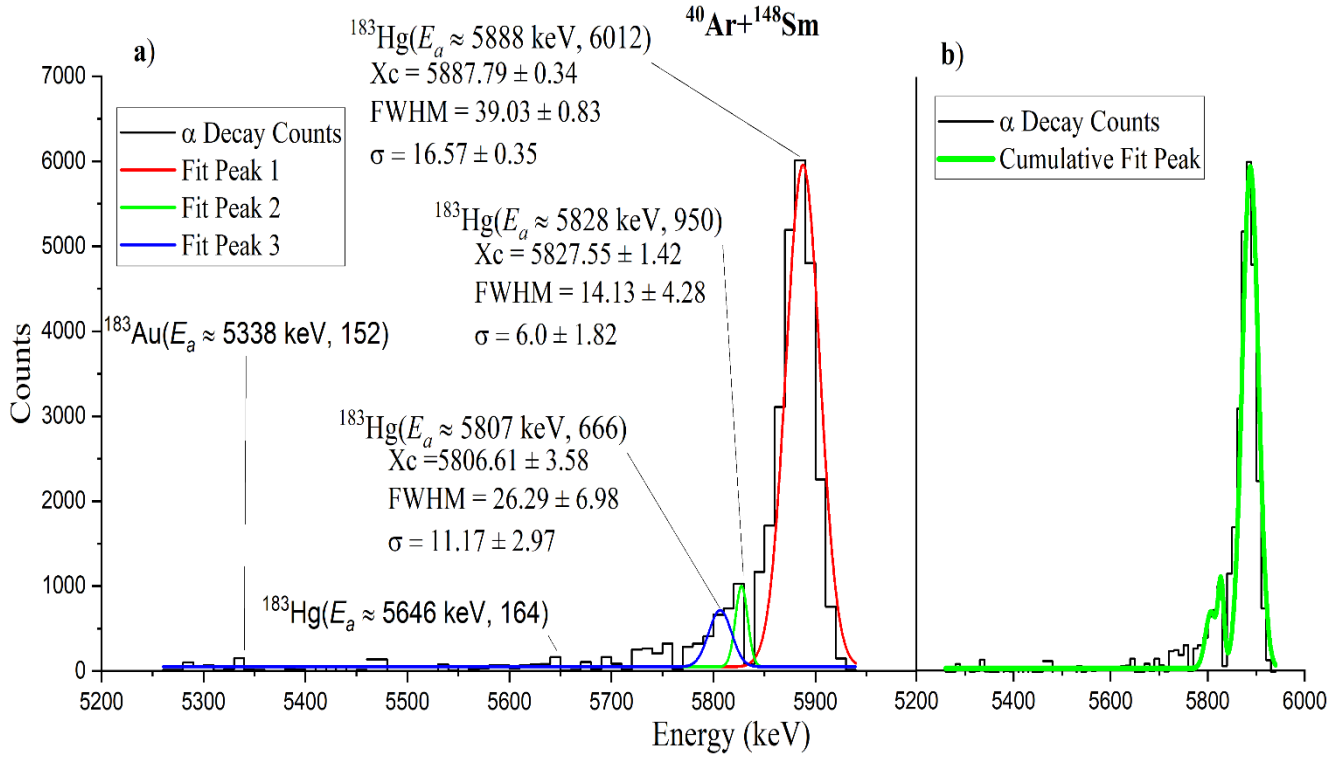

Figure 2-15: a) shows the peak analysis for individual a Decay and b) shows the cumulative fit peak.

The three primary daughters of ^{183}Hg(9.4 s) as seen in its decay chain are ^{183}Au(42.8 s), ^{179}Pt(21.1 s)

and ^{182}Pt(3.0 min). However, most of the decay observed in the spectrum are of ^{183}Hg and only one from other isotope ^{183}Au($E_a \approx 5346$ keV) was observed at 5338 keV. The rest alpha decays of ^{18}3Hg($E_a \approx 5904$ keV), ^{183}Hg($E_a \approx 5834$ keV) , ^{183}Hg($E_a \approx 5819$ keV) and ^{183}Hg($E_a \approx 5669$ keV) were peaked at 5888 keV, 5828 keV , 5807 keV and 5646 keV respectively. The GaussAmp peak fit was obtained to be very good with Adj.R^2 equal to 0.9842. The fitting for very weak peaks was not performed as seen in Figure 2-15.

2.3.5 Production of ^{184}Hg

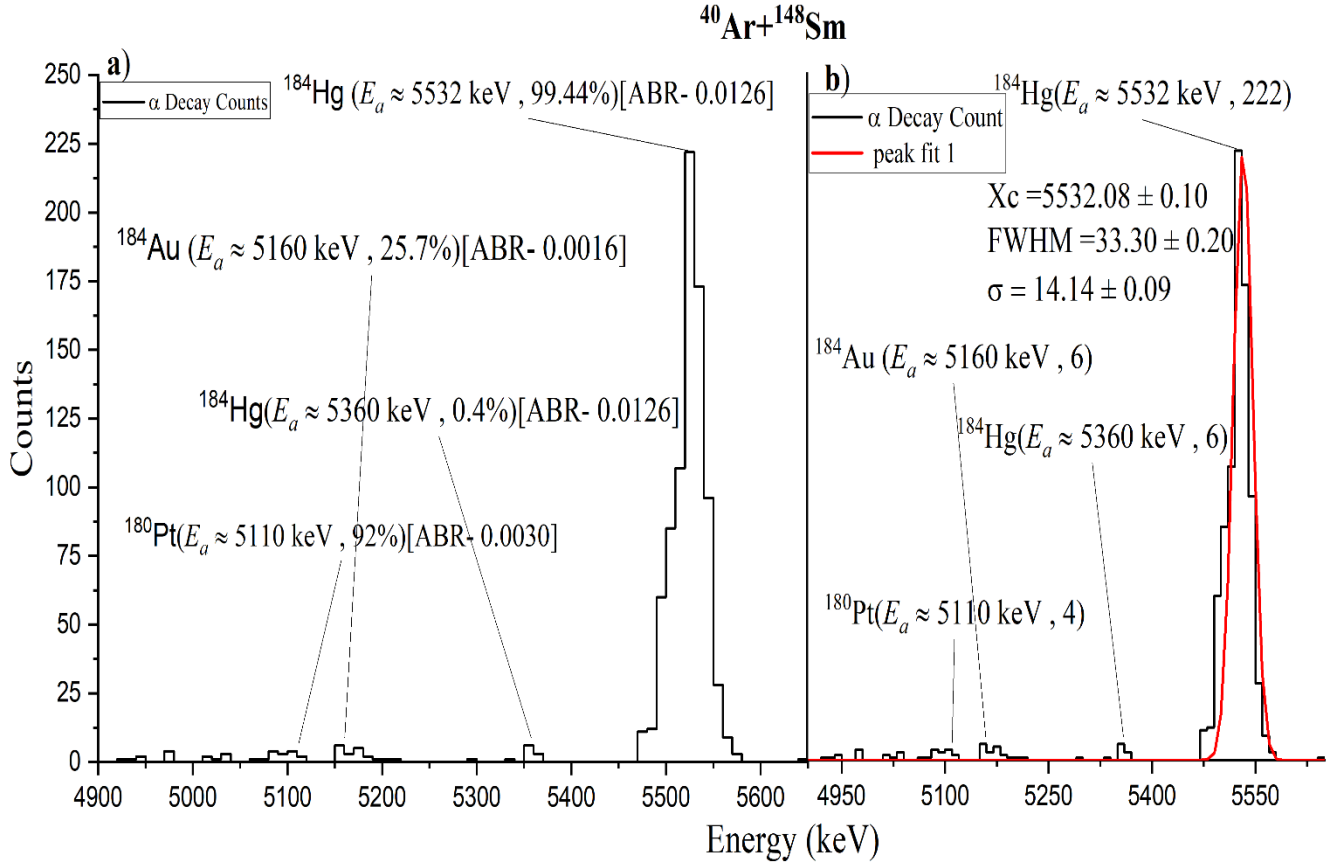

Figure 2-16: a) Shows the alpha spectrum of ^{184}Hg and its identified peaks of the spectrum along with its properties of decay. b) Peak analysis for the ^{184}Hg alpha spectrum and its peak parameters.

The production of 184Hg could be seen as really low compared to other isotopes of Hg discussed in this section which is due to very little ABR. It was really hard to distinguish peaks between the background or the alpha decay counts. However, a trend of increasing and decreasing of the counts in the data column was followed and the peaks were marked as seen in above figure 2-16 a). The most prominent alpha decay peak of 184Hg(Ea ≈ 5535 keV) was observed at 5532 keV. The alpha decay peaks for 184Au(Ea ≈ 5187 keV)(47.6 s), 184Hg(Ea ≈ 5380 keV)(30.9 s), and for 180Pt(Ea ≈ 5140 keV)(56 s) was peaked at approximately 5160 keV, 5360 keV, and 5110 keV respectively. The GaussAmp peak fit performed for a single peak as shown in figure 2-16 b) had Adj.R2 value equal to 0.8831.

2.3.6 Production of ^{185}Hg

The prominent alpha decay of ^{185}Hg($E_a \approx 5653$ keV)(49.1 s) was observed to be peaked at 5647 keV as seen in below figure 2-17 a). The other two alpha decay peaks noticed were of ^{185}Hg($E_a \approx 5569$ keV)(49.1 s) and ^{185}Au($E_a \approx 5069$ keV)(4.25 min) at energies approximately equal to 5570 keV and 5079 keV respectively. The GaussAmp peak fitting of the peaks as seen in Figure 2-17 had Adj.R^2 was obtained to be 0.9744, which is a very good fit. The standard error in the peak parameter in the weak and broader peaks came out to be high.

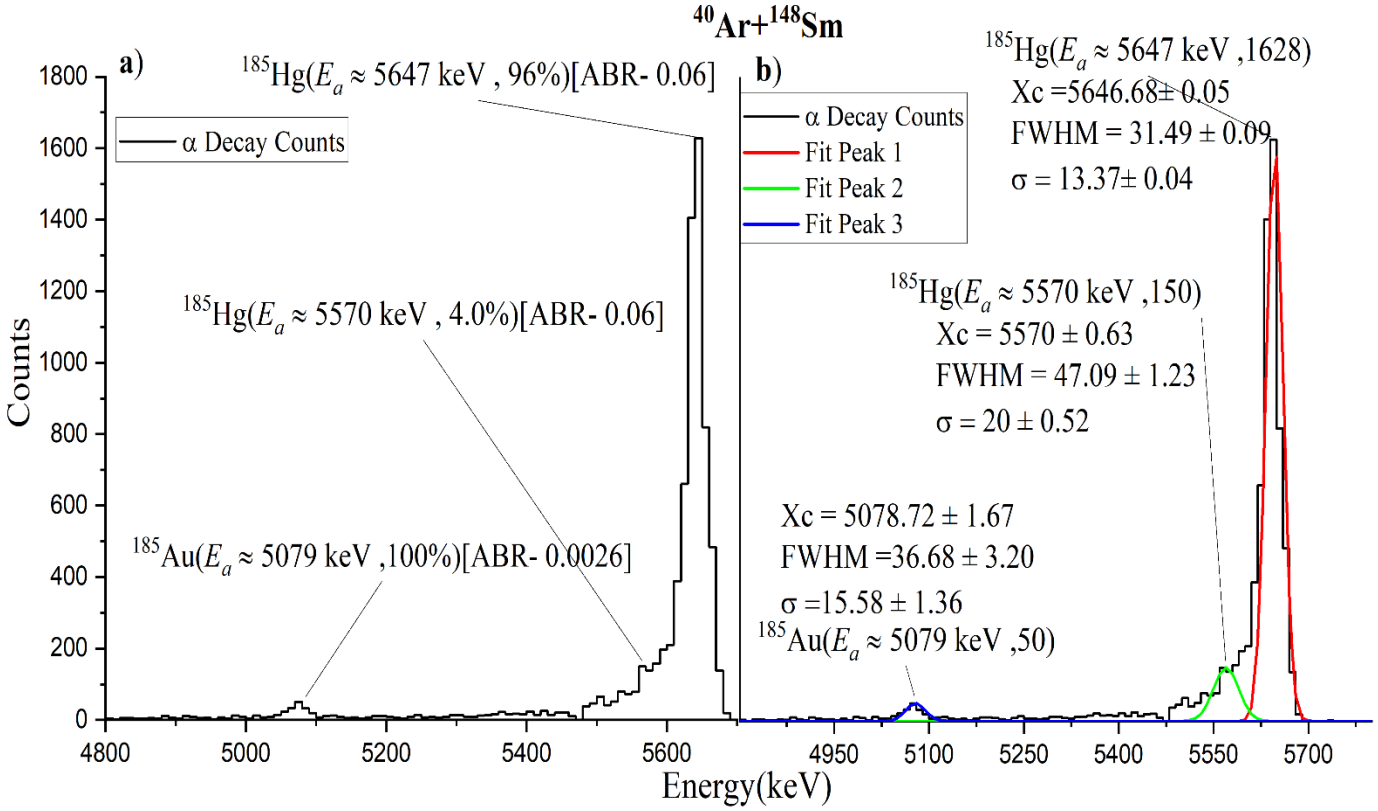

Figure 2-17: a) Shows the alpha spectrum of ^{185}Hg and its identified peaks of the spectrum along with its properties of decay. b) Peak analysis for the ^{185}Hg alpha spectrum and its peak parameters.

2.3.7 Heatmap for Hg Isotopes

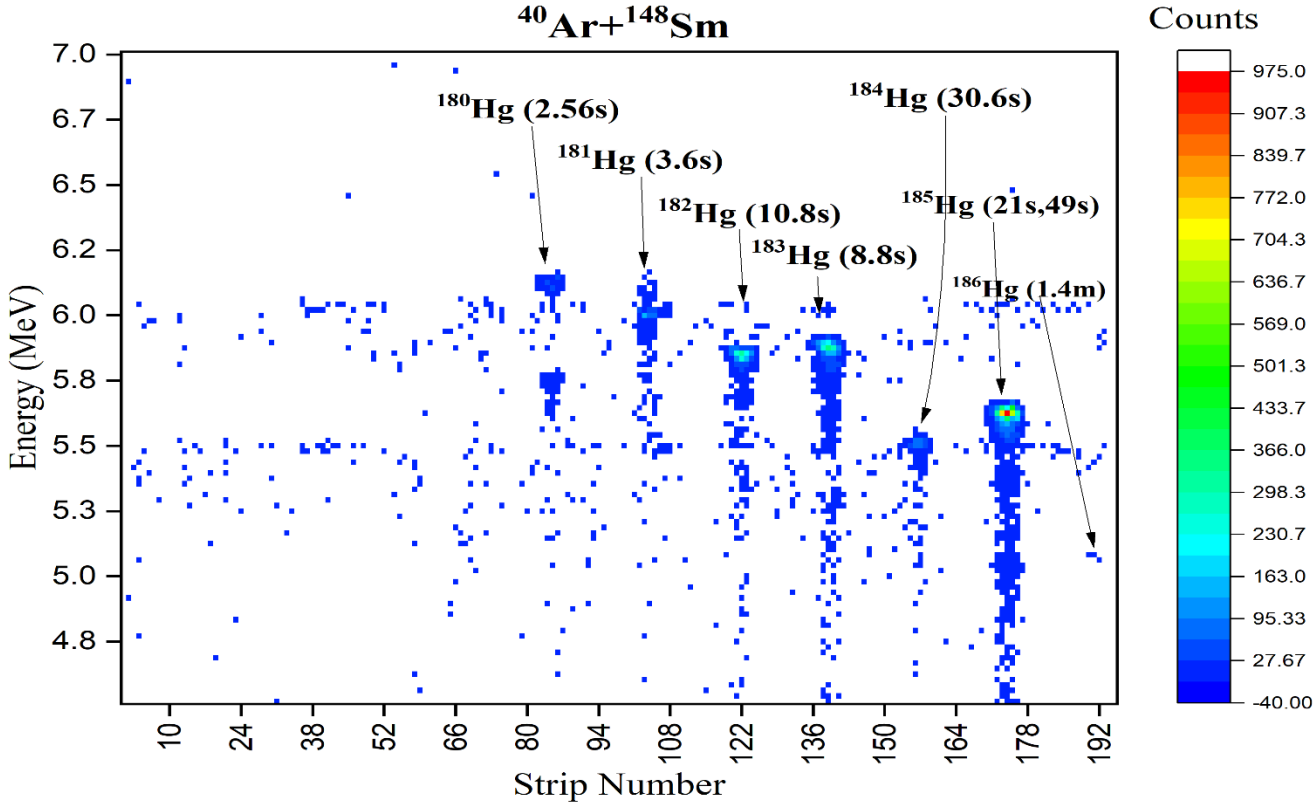

Figure 2-18: Two-dimensional energy-position graph for Hg isotopes from mass numbers 180 to 186.

Results and Conclusion.

In this project work, the data analysis performed for the Experimental data obtained from the three multinucleon transfer reactions brings out the Evidence of different Rn and Hg Isotopes produced. Data analysis included plotting and studying the alpha spectrums of different Isotopes and finding the alpha decay peaks and their corresponding energies. Which then concluded the production of a particular Isotope responsible for it. Peak parameters like FWHM, Standard deviation, and the Centre of the peak Xc (here it is Energy of decay) were founded by performing GaussAmp fit in most of all cases. Also, peak fitting was not performed for all the peaks.

By analyzing and constructing graphs for the ^{48}Ca + ^{242}Pu multinucleon transfer reaction, the highest production was obtained of ^{212}Rn isotope followed by ^{219}Rn. Opposite to that, Due to a very less lifetime of ^{218}Rn, barely any alpha decay corresponding to it was observed. Its production confirmation was done by witnessing the alpha decay from its daughter Nucleus. Also, the deviation in the alpha decay energy observed for each isotope from that given in the chart of nuclide was larger as compared to other reactions. As seen in the chart of Nuclides, the alpha branching ratio constantly decreases going from ^{201}Rn to ^{205}Rn isotope, meaning to - lower alpha decays observed and hence low production of that isotope justified by studying the alpha spectrum. These similar results could be seen while looking at the counts of alpha decay observed in their respective alpha decay spectrum for ^{40}Ar+^{166}Er reaction.

In the case of ^{40}Ar+^{148}Sm MNTR, the counts observed for the ^{182}Hg were the highest followed by ^{181}Hg and ^{183}Hg. The production of ^{184}Hg was observed to be the lowest and the difference between the minimum counts observed with the maximum peak was also high. The peaks obtained from the alpha spectrum data of Hg isotopes were very irregular in many cases, also there were so many negative counts in the data set which was neglected while plotting. The other thing noticeable was the comparison of the Two-dimensional energy position graph (Figure 2-18) with that of different alpha spectrums of Hg. As per figure 2-18, the maximum counts were of ^{185}Hg, however, that was not the case seen compared to the trend of counts seen in their alpha spectrums.

Acknowledgments

Firstly, I am highly thankful to my guide Mr. Viacheslav Vedeneev for selecting me for this project and allowing me to work for the prestigious JINR institute. It was my great pleasure performing the task given and I was greatly helped by him whenever I had problems in understanding the topic and in my project work. With his important support, I am glad that I have completed this project, Lastly, I would like to thank the Interest management team and their members for their constant support in the application process.

References.

[1] V. Y. Vedeneev *et al.*, "The current status of the MASHA setup," *Hyperfine Interact.*, vol. 238, no. 1, pp. 1–14, 2017, DOI: 10.1007/s10751-017-1395-9.

[2] E. Kugler *et al.*, "The new CERN-ISOLDE on-line mass-separator facility at the PS-Booster," *Nucl. Instruments Methods Phys. Res. Sect. B Beam Interact. with Mater. Atoms*, vol. 70, no. 1–4, pp. 41–49, Aug. 1992, DOI: 10.1016/0168-583X(92)95907-9.

[3] A. M. Rodin *et al.*, "MASHA separator on the heavy ion beam for determining masses and nuclear physical properties of isotopes of heavy and superheavy elements," *Instruments Exp. Tech.*, vol. 57, no. 4, pp. 386–393, 2014, DOI: 10.1134/S0020441214030208.

[4] M. Schadel, "Chemistry of superheavy elements.," 2016.

[5] Y. T. Oganessian and S. N. Dmitriev, "Superheavy elements in D I Mendeleev's Periodic Table," *Russ. Chem. Rev.*, vol. 78, no. 12, pp. 1077–1087, 2009, DOI: 10.1070/rc2009v078n12abeh004096.